GMR
The Original

SUSTAINABLE GREEN FABRICATION OF STARCH/PVA/CuO-NPs ELECTROSPUN NANOSCAFFOLDS FROM *Turbinaria conoides* EXTRACT FOR ENHANCED ANTICANCER ACTIVITY ON HT-29 AND MCF-7 CELLS

Gopika Mohanakumar[1], Sinega NS[2], Alagendran Subbarayalu[3]*

[1]Saveetha Medical College & Hospital (SMCH), Saveetha Institute of Medical and Technical Sciences (SIMATS), Thandalam, Chennai, Tamil Nadu 602105, India. gopikamohanakumar2307@gmail.com
[2]Department of Pathology, Saveetha Medical College and Hospital, Saveetha Institute of Medical And Technical Sciences (SIMATS), Thandalam, Chennai-602105, Tamil Nadu, India. Email: sinegasivasamy95@gmail.com; ORCID: https://orcid.org/0009-0005-1788-5401.
[3]Clinical Neuroscience and Phytomedicine Laboratory, Department of Research, Saveetha College of Nursing (SCON), Saveetha Institute of Medical and Technical Sciences (SIMATS), Chennai 602105, Tamil Nadu, India. Email: proteinblg@gmail.com; alagendrans.scon@saveetha.com. ORCID: https://orcid.org/0009-0009-0749-7180.
*Correspondence: proteinblg@gmail.com; alagendrans.scon@saveetha.com (A.S.)

ABSTRACT
This study presents a novel approach for fabricating starch/polyvinyl alcohol (PVA) electrospun nanoscaffolds integrated with biogenically synthesized copper oxide (CuO) nanoparticles derived via ultrasonic-assisted extraction from the brown marine macroalga *Turbinaria conoides*. Comprehensive physicochemical analyses confirmed successful nanoparticle synthesis and uniform incorporation within the polymer matrix, evidenced by UV-Vis spectroscopy, Fourier-transform infrared spectroscopy (FTIR), X-ray diffraction (XRD), Scanning electron microscopy (SEM), and thermal stability assessments. The CuO nanoparticles exhibited characteristic monoclinic crystal structures and nanoscale dimensions, while the nanoscaffolds demonstrated enhanced thermal stability and homogenous fibrous morphology. Dynamic light scattering (DLS) and zeta potential studies revealed moderate colloidal stability of CuO NPs. Importantly, the fabricated nanocomposites displayed potent, dose-dependent cytotoxicity against HT-29 and MCF-7 cancer cell lines, surpassing the effects of both the raw algal extract and CuO nanoparticles alone. These findings underscore the promising potential of the starch/PVA/CuO nanoscaffolds as effective anticancer agents, warranting further investigation into their therapeutic mechanisms and *in vivo* efficacy for cancer treatment applications.

KEYWORDS: *Turbinaria conoides*, Green synthesis, CuO nanoparticles, Starch/PVA/CuO-NPs nanoscaffolds, Anticancer activity.

1. INTRODUCTION

Nanotechnology has revolutionized the fields of material science and biomedical engineering by enabling the design and fabrication of novel nanoscale materials with enhanced properties and multifunctionality [1]. Among these, metal oxide nanoparticles have gained significant attention for their unique physicochemical characteristics, including high surface area, catalytic activity, and biological effects [2]. In particular, copper oxide nanoparticles (CuO NPs) have emerged as promising candidates in biomedical applications due to their notable antimicrobial, anti-inflammatory, and anticancer properties [3]. However, conventional chemical and physical methods of synthesizing CuO NPs often involve toxic reagents, high energy consumption, and environmental hazards, limiting their biomedical applicability [3]. This challenge has led to increased interest in developing green synthesis routes that employ biological resources for the eco-friendly production of nanoparticles [4].

Biogenic synthesis of nanoparticles using plant and algal extracts offers a sustainable and cost-effective alternative by harnessing the inherent reducing, capping, and stabilizing agents present in natural biomolecules such as polyphenols, flavonoids, proteins, and polysaccharides [5]. Marine macroalgae, commonly known as seaweeds, represent a prolific reservoir of bioactive compounds with diverse chemical structures and biological functions [6]. Among these, *Turbinaria conoides*, a brown marine macroalga abundantly found along the coastal regions of India, has demonstrated a rich profile of polysaccharides, phenolic compounds, and antioxidants [7]. These biomolecules not only facilitate the rapid reduction of metal ions but also enhance the stability and functionality of the synthesized nanoparticles [8]. Despite this potential, few studies have explored the ultrasonic-assisted

extraction of *T. conoides* phytoconstituents specifically for the green synthesis of CuO NPs, which could improve extraction efficiency and nanoparticle quality by promoting better cell wall disruption and metabolite release [9].

In parallel, the development of nanofibrous scaffolds for biomedical applications, particularly in tissue engineering and drug delivery, has witnessed remarkable advancements through electrospinning technology [10]. Electrospinning enables the fabrication of continuous fibers with diameters ranging from the nanometer to micrometer scale, closely mimicking the extracellular matrix (ECM) architecture [11]. Such scaffolds provide a highly porous and biocompatible environment conducive to cell attachment, proliferation, and differentiation [12]. Polyvinyl alcohol (PVA), a synthetic hydrophilic polymer, has been widely used in electrospinning due to its excellent film-forming ability, biocompatibility, and mechanical strength [13]. However, PVA alone lacks bioactivity and rapid biodegradability. To overcome these limitations, natural polymers like starch are incorporated to improve biodegradability, enhance biological interactions, and reduce the reliance on synthetic polymers [14]. Starch, a renewable polysaccharide, is especially attractive owing to its abundance, low cost, and inherent biocompatibility, making it an ideal candidate to form composite scaffolds with PVA [15].

Integrating biogenic metal oxide nanoparticles within polymeric nanofibrous matrices offers a promising strategy to develop multifunctional scaffolds that combine mechanical integrity with therapeutic activity [16]. Embedding CuO NPs into starch/PVA electrospun scaffolds can potentially impart anticancer and antimicrobial functionalities, while maintaining favorable physicochemical properties essential for biomedical use [17]. However, achieving uniform nanoparticle dispersion and stable incorporation without compromising fiber morphology or scaffold performance remains a critical challenge [16]. Employing ultrasonic-assisted green synthesis of CuO NPs from *T. conoides* extract and their subsequent incorporation into starch/PVA nanofibers represents an innovative approach to address these issues [17]. This methodology leverages the synergistic advantages of eco-friendly nanoparticle synthesis, efficient phytochemical extraction, and advanced electrospinning fabrication to yield functional nanoscaffolds with potential anticancer efficacy [18].

Cancer remains a leading cause of mortality worldwide, and conventional chemotherapy often suffers from severe side effects and drug resistance [19]. Nanomaterial-based therapies offer targeted and controlled delivery options that could enhance therapeutic indices and minimize adverse reactions [20]. CuO NPs have been reported to induce reactive oxygen species (ROS) generation selectively in cancer cells, triggering apoptosis and inhibiting tumor progression [21]. By embedding these nanoparticles within biodegradable nanoscaffolds, a localized and sustained anticancer effect can be achieved, which may improve treatment outcomes and reduce systemic toxicity [22]. Despite these promising prospects, comprehensive studies on the physicochemical characterization, biological compatibility, and anticancer activity of such biogenic CuO NP-incorporated starch/PVA scaffolds are scarce, especially when the nanoparticles are synthesized using marine macroalgal extracts [23].

Therefore, this study aims to develop a novel starch/PVA electrospun nanofibrous scaffold embedded with CuO NPs synthesized via an ultrasonic-assisted green method using *T. conoides* extract. The objectives include the optimization of phytochemical extraction from *T. conoides* by ultrasonication, the eco-friendly biosynthesis of CuO NPs [9], and the fabrication of uniform composite nanoscaffolds through electrospinning [24]. Extensive physicochemical characterization techniques such as UV–Vis spectroscopy, Fourier-transform infrared spectroscopy (FTIR), X-ray diffraction (XRD), Scanning electron microscopy (SEM), Thermogravimetric analysis (TGA), and particle size analysis are employed to elucidate nanoparticle formation, structural integration, fiber morphology, thermal stability, and colloidal properties [25]. Moreover, the anticancer potential of the synthesized scaffolds is evaluated against human colon (HT-29) and breast (MCF-7) cancer cell lines using standard cytotoxicity assays [26].

The innovative combination of marine macroalgal biogenic synthesis and starch/PVA electrospun scaffolds presented in this work offers an environmentally sustainable and potentially effective platform for anticancer applications. The integration of bioactive CuO NPs derived from *T. conoides* extract within a biocompatible polymer matrix addresses current challenges in nanomedicine related to toxicity, stability, and multifunctionality. This research could pave the way for developing next-generation nanomaterials for cancer therapeutics and tissue engineering, contributing to the broader goals of green nanotechnology and precision medicine.

2. MATERIALS AND METHODS

2.1. Chemicals and reagents

For this study, *T. conoides*, a brown seaweed native to the coastal region of Rameswaram, Tamil Nadu, India, was selected for the green synthesis of CuO NPs. Copper (II) sulfate pentahydrate, of analytical purity, served as the metal precursor. PVA, having an approximate molecular weight of 115,000 g/mol, and starch were used to produce nanofibrous scaffolds via electrospinning using a HOLMARC HO-NFES-040 system. All required solvents and chemical agents, sourced from Merck and Sigma-Aldrich, were of analytical grade to ensure experimental

reproducibility. The synthesized materials underwent detailed physicochemical characterization and were further assessed for their anticancer efficacy through established bioassays.

2.2. Collection and preparation of algal biomass

Fresh specimens of *T. conoides* were collected manually from the intertidal zones along the Rameswaram coast. The samples were immediately transferred to the laboratory in ice-filled containers. Surface impurities such as epiphytes and sediments were removed through thorough rinsing with tap water, followed by multiple washes using distilled water to eliminate salt residues. Approximately 100 g of cleaned algal thalli were chopped into small sections and air-dried at room temperature for 14 days. Once completely dried, the algal material was finely ground and stored in airtight containers for further extraction and nanoparticle synthesis.

2.3. Ultrasonic extraction of phytoconstituents

To extract phytochemicals, 2 g of the powdered algal biomass was added to 50 mL of Milli-Q water in a 100 mL borosilicate container. The suspension underwent ultrasonic-assisted extraction using a LABQUEST ultrasonic cleaner (Borosil, Serial No. 941032329018) at 60°C for 45 minutes to enhance cellular disruption and metabolite release. The extract was filtered through Whatman No. 1 filter paper to remove particulate matter. The clear extract was refrigerated at 10°C until further use, and a portion was freeze-dried to obtain a stable powdered extract suitable for nanoparticle synthesis [27, 28].

2.4. Eco-friendly synthesis of CuO NPs

For biosynthesis, 50 mL of 0.1 M copper sulfate solution was combined with 10 mL of algal extract (10 mg dry weight equivalent) at a 5:1 ratio. This solution was continuously stirred at 650 rpm and maintained at 60°C for 2 hours using a magnetic stirrer with temperature control. A visible color change from deep blue to bluish-green indicated successful reduction of copper ions by the algal phytochemicals. The resultant nanoparticles were washed three times with double-distilled water to remove unreacted components, then freeze-dried for 48 hours to obtain a powdered form of CuO NPs [29].

2.5. Fabrication of starch/PVA/CuO NP nanofiber scaffolds

To fabricate nanoscaffolds, a 15% (w/w) aqueous PVA solution was prepared by dissolving the polymer in Milli-Q water with constant stirring at 50°C. After complete solubilization, 100 mg of starch and synthesized CuO NPs were incorporated into the solution. This mixture was stirred for an additional 2.5 hours at the same temperature to ensure homogenous dispersion. The final blend was transferred into a syringe with a 0.84 mm stainless steel needle for electrospinning on a HOLMARC HO-NFES-040 unit. The setup operated at room temperature with optimized parameters: 11.5 kV voltage, 12.3 cm needle-to-collector distance, and 0.4 mL/h flow rate. Electrospinning was carried out for 6 to 8 hours to form uniform nanofibers, which were collected and stored in desiccators for later characterization [30-32].

2.6. Physicochemical characterization

2.6.1. UV–visible spectroscopy

UV–Vis spectral analysis was performed using a VIS SPEC V-730 spectrophotometer to assess the optical features of algal extract, CuO NPs, and composite nanoscaffolds. Absorbance was recorded over the 200 to 800 nm range using deionized water as a blank. Specific absorption bands between 270 and 300 nm confirmed nanoparticle synthesis and scaffold incorporation [33].

2.6.2. FTIR spectroscopy analysis

FTIR spectroscopy was conducted using a PerkinElmer Spectrum Two in ATR mode to analyze functional groups and molecular interactions. Each sample was scanned in the 4000–400 cm^{-1} range with 64 scans and a 4 cm^{-1} resolution. Peaks attributed to hydroxyl, carbonyl, amide, and metal–oxygen bonds verified both phytochemical presence and nanoparticle inclusion [34].

2.6.3. XRD analysis

Crystalline structure and phase analysis of CuO NPs and their integration within scaffolds were assessed using a Bruker D8 Advance diffractometer with CuKα radiation (λ = 1.5406 Å). Scans ranged from 5° to 90° 2θ at 40 kV and 40 mA, with a 0.029649° step size. Distinct peaks representing monoclinic CuO confirmed crystallinity; broadened peaks in the nanocomposites indicated good nanoparticle dispersion [35].

2.6.4. SEM analysis

Surface morphology and fiber uniformity were examined via a JEOL JSM-IT800 NANO SEM. Samples were coated with a thin layer of gold to reduce charging. The SEM images demonstrated even fiber diameters and uniform CuO NP distribution, affirming successful electrospinning [36].

2.6.5. TGA

TGA was used to assess the thermal properties using a PerkinElmer TGA 8000. About 5 mg of each sample was heated from room temperature to 550°C at 15°C/min in a nitrogen atmosphere. The thermograms illustrated multiple degradation stages, highlighting moisture loss, polymer decomposition, and enhanced thermal stability due to nanoparticle reinforcement [37].

2.6.6. Particle size and zeta potential measurements

Size and surface charge of CuO NPs were determined using a Malvern Zetasizer Ultra. Hydrodynamic diameter was measured using Dynamic Light Scattering (DLS), while zeta potential assessed colloidal stability. Nanoparticles with zeta potential values beyond ±30 mV were deemed stable for biological applications [38].

Characterization data are publicly available on Mendeley Data (DOI: 10.17632/mmyv8mmkbx.2).

2.7. *In vitro* anticancer activity

2.7.1. Cell lines (HT-29 and MCF-7) procurement and culture

Human colon cancer (HT-29) and breast cancer (MCF-7) cell lines were obtained from the National Center for Cell Science (NCCS), Pune, India. Cells were cultured following standard protocols in Minimum Essential Medium (MEM) with 10% fetal bovine serum (FBS) at 37°C under 5% CO_2 in a humidified incubator [26].

2.7.2. MTT assay for cell viability

Cells were seeded in 96-well plates at 5 x 10^5 cells/well and allowed to adhere overnight. They were then exposed to varying concentrations (6.25, 12.5, 25, 50, 100 µg/mL) of algal extract, CuO NPs, and starch/PVA/CuO-NP nanoscaffolds for 24 hours. Following incubation, MTT reagent was added and the cells were incubated for an additional 4 hours. Formazan crystals formed were solubilized with 200 µL DMSO, and absorbance was measured at 570 nm using a microplate reader. Experiments were repeated thrice independently for accuracy. The mean optical density and standard deviation were calculated to interpret cytotoxicity effects [39].

2.8. Statistical analysis

Statistical evaluations were performed using SPSS v25.0 and GraphPad Prism v9.0. Data from triplicate experiments were expressed as mean ± standard deviation. One-way ANOVA with appropriate post hoc tests (Tukey's or Dunnett's) determined group differences, with significance set at $p < 0.05$. Pearson's correlation and Shapiro–Wilk normality tests were also applied. If needed, data were log-transformed to meet normality criteria. All results were analyzed within a 95% confidence level to ensure statistical rigor [40].

3. RESULTS AND DISCUSSION

3.1. UV-visible spectroscopy

The UV–Visible absorption spectra of *T. conoides* aqueous extract, the biosynthesized CuO NPs, and the CuO-loaded starch/PVA nanoscaffolds were recorded using a JASCO V-730 spectrophotometer within a wavelength range of 200–800 nm (Fig. 1). The crude seaweed extract exhibited broad absorption peaks in the lower wavelength region, which is typical for compounds such as flavonoids and polyphenols that absorb ultraviolet light due to their conjugated π-electron structures.

The biosynthesized CuO NPs showed a distinct, sharp absorption peak in the 270–300 nm range, indicative of surface plasmon resonance (SPR). This SPR phenomenon arises from the collective oscillation of conduction electrons on the nanoparticle surface excited by light. The clear SPR peak confirms the successful biosynthesis of CuO NPs from Cu2+ ions, mediated by the seaweed's bioactive compounds.

When embedded within starch/PVA nanofibers, the CuO NPs caused subtle spectral shifts and broadening of absorption peaks relative to pure CuO NPs. These spectral changes imply interactions at the molecular level, likely hydrogen bonding or van der Waals forces, between CuO NPs and the polymer chains. This confirms the effective encapsulation and uniform dispersion of CuO NPs throughout the scaffold. All measurements were performed in triplicate for reliability, using deionized water as the baseline reference to remove background noise [41-43].

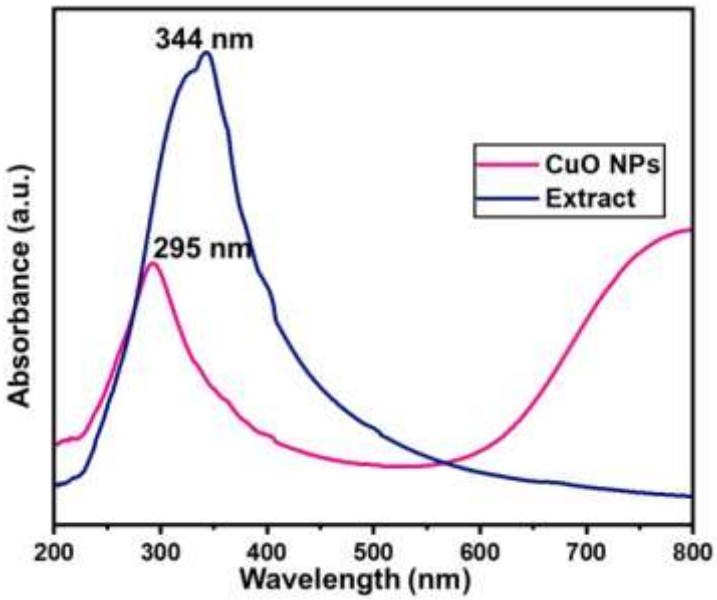

Fig. 1. UV–Visible spectral profiles of algal extract and CuO NPs.

3.2. FTIR spectroscopy analysis

FTIR spectroscopy was employed to elucidate the functional groups involved in nanoparticle stabilization and their interaction with the polymer matrix. The spectra of CuO NPs and CuO-loaded scaffolds were recorded via a PerkinElmer Spectrum Two FTIR spectrometer in ATR mode, scanning between 4000 and 400 cm^{-1} at 4 cm^{-1} resolution over 64 scans.

The FTIR spectrum of the CuO NPs (Fig. 2) revealed characteristic Cu–O stretching vibrations at 590.53 cm^{-1} and 464.53 cm^{-1}, confirming copper oxide formation. Additional peaks at 801.66 cm^{-1} corresponded to C–H bending, while 1015.22 cm^{-1} and 1065.56 cm^{-1} were assigned to C–O stretching modes. The absorption at 1511.28 cm^{-1} represented aromatic C=C or N–H bending vibrations. A broad O–H stretching band appeared at 3166.88 cm^{-1}, indicating the presence of phytochemicals from the algae adsorbed onto the nanoparticle surface. In the CuO-loaded starch/PVA scaffold, the FTIR spectra showed new and shifted peaks confirming nanoparticle incorporation. The Cu–O band appeared at 603.51 cm^{-1}, reaffirming CuO presence. Other prominent bands included 843.42 cm^{-1} (C–H bending), 913.12 cm^{-1} (C–O–C stretching), and 1089.99 cm^{-1} (C–O stretching), characteristic of polysaccharide and ether groups. Strong vibrations at 1425.37 cm^{-1} and 2923.53 cm^{-1} were linked to C–H groups, while peaks at 1711.84 cm^{-1} and 1732.70 cm^{-1} indicated ester and carbonyl groups from PVA. The broad O–H stretch at 3296.86 cm^{-1} suggested hydrogen bonding, supporting a stable interaction network between polymer and nanoparticles [44-49].

3.3. XRD analysis

XRD was performed to assess the crystalline structure and the integration of CuO NPs within the nanoscaffolds. A Bruker D8 Advance diffractometer with CuKα radiation (λ = 1.5406 Å) was used at 40 kV and 40 mA, scanning 2θ from 5° to 90° with a step size of 0.029649° (Fig. 3).

The diffraction pattern of the CuO NPs displayed sharp, well-defined peaks characteristic of a monoclinic crystal phase, consistent with JCPDS card No. 48-1548. Notable reflections were observed at 15.666°, 16.451°, 17.368°, 20.181°, 24.173°, 26.071°, 28.492°, 31.764°, 32.614°, 35.035°, 38.242°, and 47.468°. The most intense peak at 26.071° corresponded to a d-spacing of 3.41519 Å and a narrow full width at half maximum (FWHM) of 0.100°, suggesting small crystallite sizes.

The XRD pattern of the CuO-loaded starch/PVA scaffold showed semi-crystalline characteristics. Peaks at 11.332°, 19.284°, 21.272°, 23.481°, 29.372°, 30.771°, 35.778°, 39.533°, and 47.559° were recorded. The strong reflection at 29.372° (d = 3.03842 Å, FWHM = 0.170°) indicated contributions from the polymer matrix. CuO-specific peaks at 30.771° and 35.778° confirmed nanoparticle retention within the scaffold. Peak broadening and shifts suggest reduced crystallite size and internal strain caused by polymer–nanoparticle interactions. The monoclinic phase of CuO remained unchanged, demonstrating that its crystal structure was preserved after embedding [50-54].

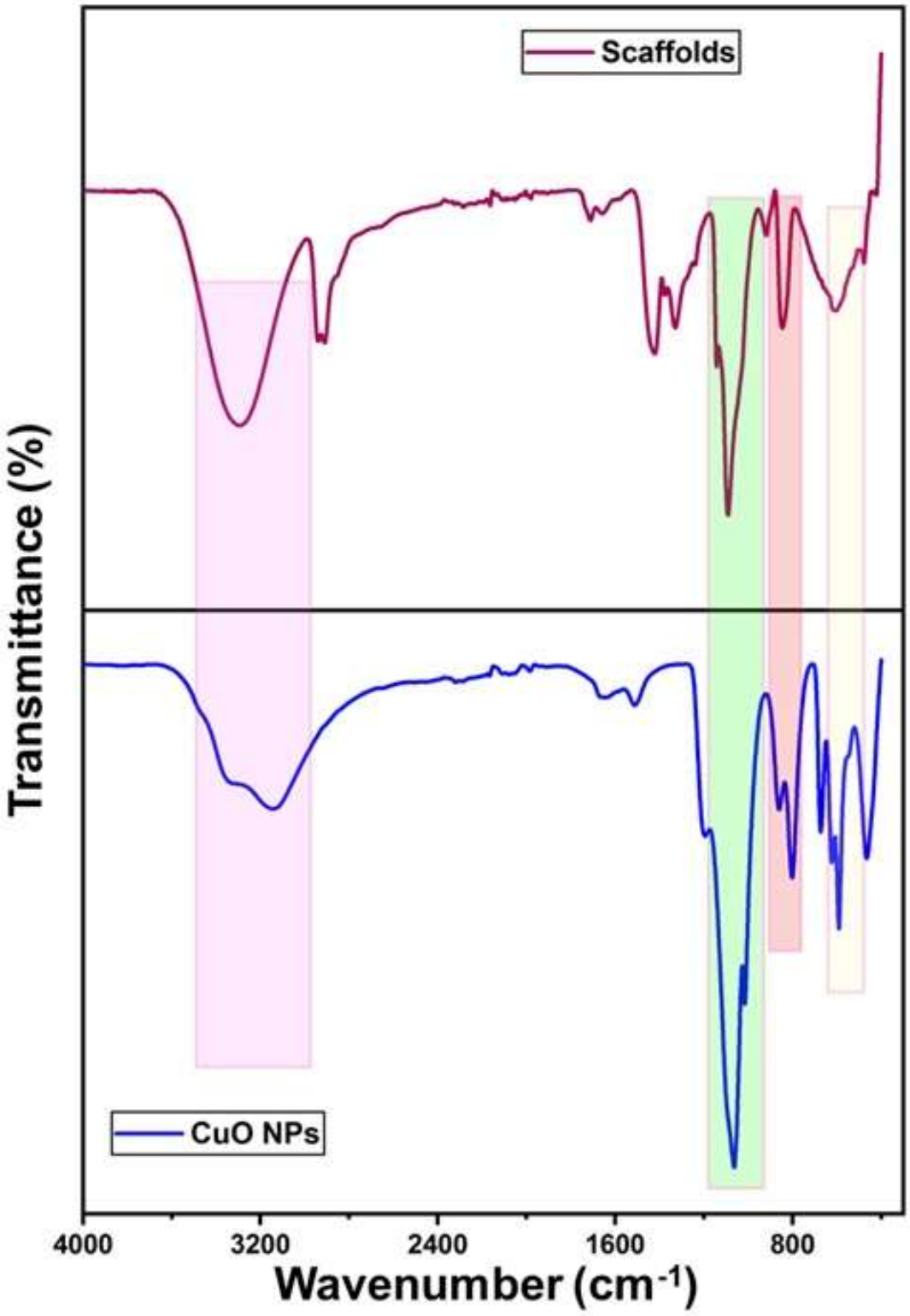

Fig. 2. FTIR spectra of CuO NPs and their incorporation into nanoscaffolds.

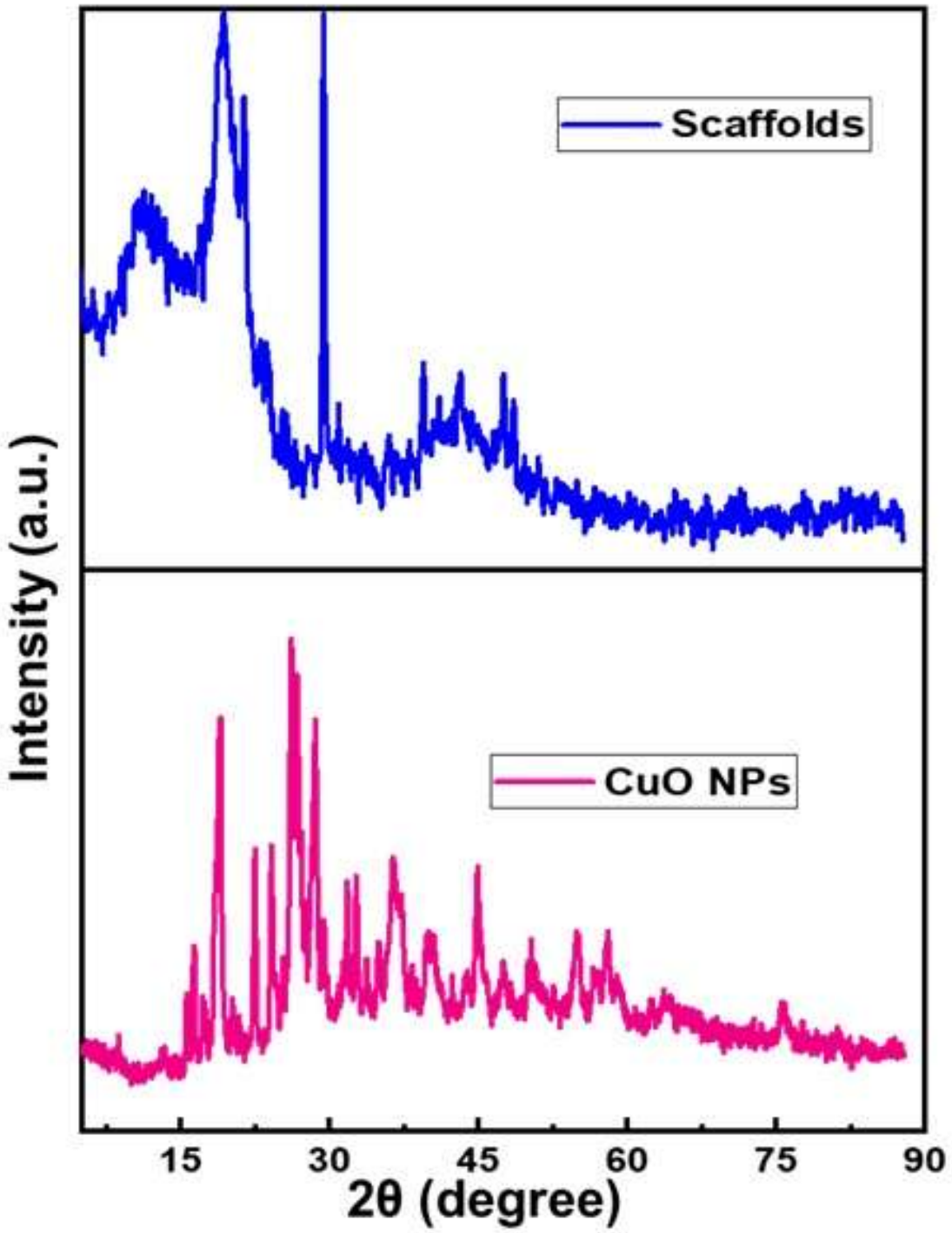

Fig. 3. XRD patterns of synthesized CuO NPs and CuO-loaded scaffolds.

3.4. SEM analysis

Surface morphology of CuO NPs and nanoscaffolds was examined using a JEOL JSM-IT800 NANO scanning electron microscope. Prior to imaging, samples were coated with gold to enhance electrical conductivity.

SEM micrographs of CuO NPs revealed predominantly spherical particles with occasional irregular shapes, sized between 60 and 90 nm. Some degree of aggregation was observed, likely due to the high surface energy of nanoparticles causing mutual attraction. SEM images of CuO-starch/PVA scaffolds (Fig. 4) displayed uniform fibrous networks with fiber diameters ranging from 90 to 110 nm. The fibers exhibited smooth surfaces and interconnected porosity, advantageous for applications such as drug delivery and tissue engineering by promoting cell adhesion and nutrient transport.

CuO NPs appeared well embedded within the fibers, distributed evenly with minimal aggregation, indicating effective incorporation through electrospinning. The consistent nanoparticle dispersion and uniform fiber formation demonstrate optimized processing parameters for fabricating stable, functional nanocomposite scaffolds [55-59].

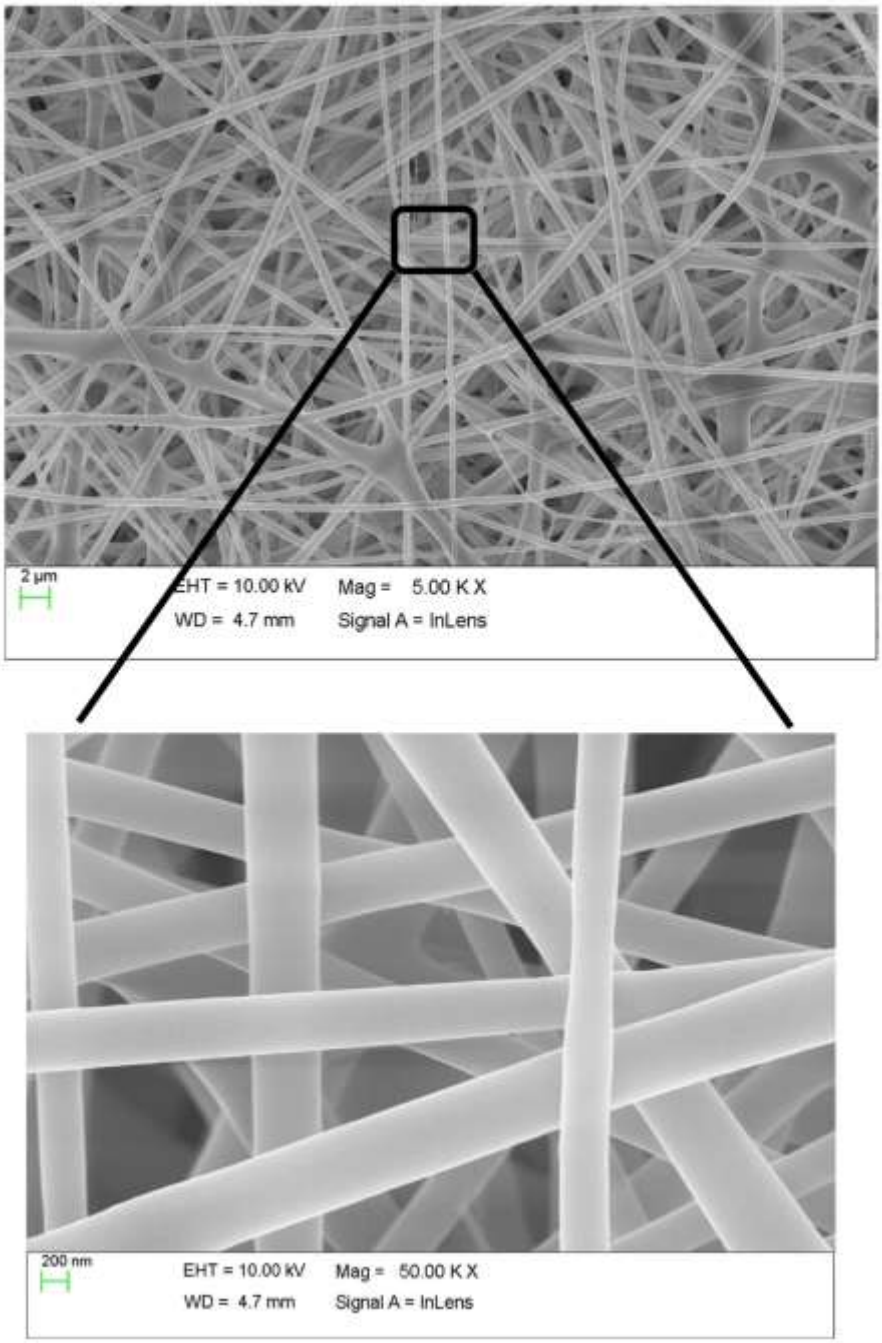

Fig.4. SEM analysis of starch/PVA/CuO-NPs nanoscaffolds

3.5. TGA

Thermal stability of CuO-loaded nanofibers was analyzed with a PerkinElmer TGA 8000 instrument. A 7.685 mg sample was heated from 30°C to 550°C at 15°C/min under nitrogen atmosphere (Fig. 5). The thermogram revealed two distinct degradation phases. The first started at 326.78°C and peaked at 381.60°C, corresponding to a mass loss of 34.960%, associated with decomposition of starch, PVA, and volatile organics. The second phase commenced at 438.61°C, reaching a maximum at 459.06°C, with an additional 4.679% weight loss attributed to degradation of residual organic materials and bioactives bound to CuO. Compared to pure starch/PVA scaffolds, the CuO-containing composites exhibited delayed thermal degradation onset, demonstrating enhanced thermal stability. This effect is attributed to the inorganic CuO restricting polymer chain mobility and acting as a thermal barrier. The derivative thermogravimetry (DTG) further clarified these transitions. Minimal residual mass at

550°C indicated nearly complete organic decomposition, with CuO functioning as a thermal stabilizer within the matrix [60-64].

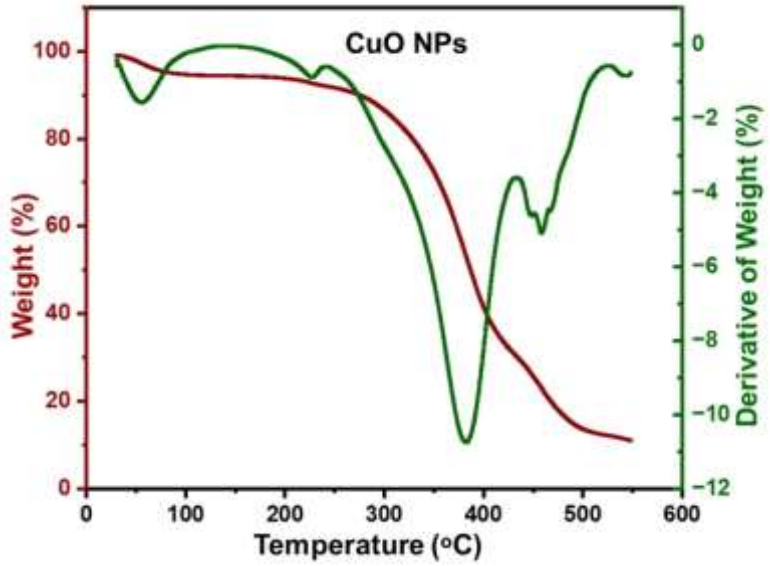

Fig. 5. Thermal degradation behavior of CuO-incorporated nanoscaffolds.

3.6. Zeta potential and particle size analysis

DLS and zeta potential measurements were carried out using a Malvern Zetasizer Ultra to determine particle size distribution and surface charge of CuO NPs. The hydrodynamic diameter distribution showed a predominant peak at 68.12 nm (Fig. 6), consistent with SEM size observations. The polydispersity index (PDI) was 0.5717, indicating moderate heterogeneity in particle sizes.

Zeta potential analysis revealed a primary surface charge of -11.39 mV with minor peaks at -42.6 mV and -12.28 mV (Fig. 7). The main zeta value suggests limited electrostatic repulsion between particles, allowing some aggregation potential over time. However, the presence of a more negatively charged fraction implies partial colloidal stability. Overall, the system's zeta potential is below the ±30 mV threshold generally regarded as indicative of strong stability. Conductivity was measured at 0.06892 mS/cm, and the count rate was 3.27×10^4 kcps, supporting reasonable dispersion quality. For enhanced long-term colloidal stability in biomedical contexts, further surface modification or stabilizing agents may be necessary. These results provide critical insights into the stability and applicability of CuO NPs for biomedical use [65-68].

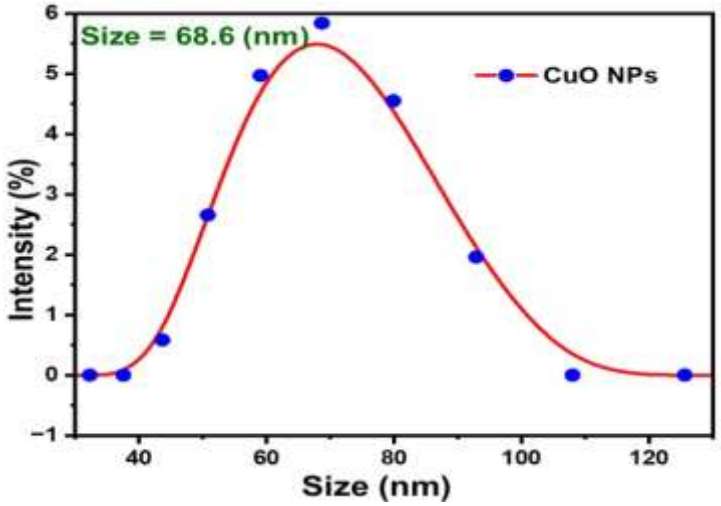

Fig.6. DLS particles size analysis of CuO NPs

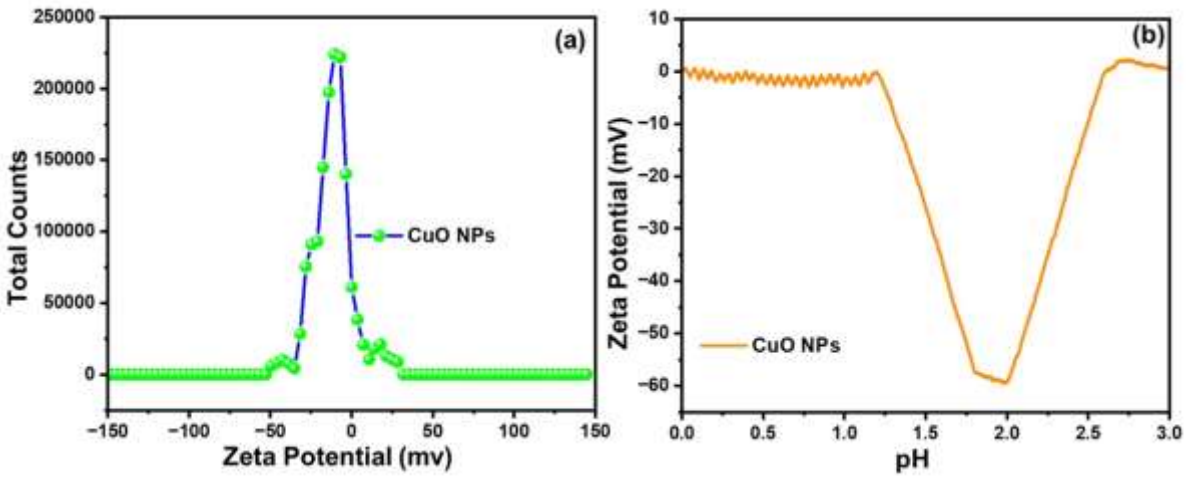

Fig.7. Zeta-potential analysis of CuO NPs

3.7. Anticancer activity analysis

The *in vitro* anticancer activity of the algal extract, CuO NPs, and starch/PVA/CuO-NPs nanoscaffolds was evaluated against HT-29 (human colon adenocarcinoma) and MCF-7 (breast cancer) cell lines using the MTT assay. Cell viability was measured at concentrations ranging from 6.25 to 100 µg/mL, with untreated cells (0 µg/mL) serving as the control (100% viability).

Against HT-29 cells, the algal extract exhibited moderate cytotoxicity, reducing cell viability from 93.5% at 6.25 µg/mL to 32.25% at 100 µg/mL, with an estimated IC_{50} value of approximately 35 µg/mL. CuO NPs demonstrated stronger activity, decreasing viability from 78.5% to 21.83% over the same concentration range, yielding an IC50 of about 18 µg/mL. The starch/PVA/CuO-NPs nanoscaffolds were the most effective, showing a sharp decline in viability from 74.9% at 6.25 µg/mL to 14.88% at 100 µg/mL, with an IC50 of approximately 12 µg/mL.

Similar trends were observed in MCF-7 cells. The algal extract reduced viability from 95.3% to 46.05%, with an IC50 of around 40 µg/mL. CuO NPs exhibited greater potency, lowering viability from 84.8% to 37.47% and achieving an IC50 of about 22 µg/mL. Once again, the nanoscaffolds displayed the highest efficacy, reducing viability from 78.4% to 24.42% and producing an IC50 of roughly 15 µg/mL.

These findings highlight the dose-dependent anticancer activity of all tested compounds, with the starch/PVA/CuO-NPs nanoscaffolds emerging as the most potent. Their superior cytotoxicity compared to CuO NPs and the algal extract suggests potential for further development as an anticancer therapeutic. Future studies should explore their mechanisms of action and *in vivo* performance to validate these promising results [69-72].

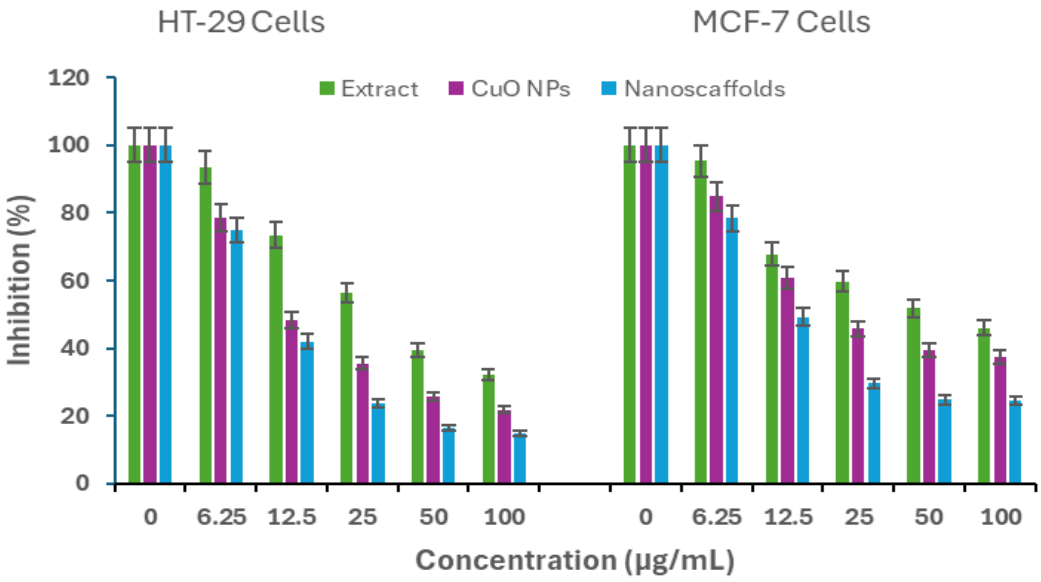

Fig.8. Anticancer activity analysis of algal extract, CuNPs and starch/PVA/CuONPs nanoscaffolds

5. CONCLUSION

This study successfully demonstrated the green synthesis of CuO NPs using *T. conoides* extract through an ultrasonic-assisted method and their effective incorporation into starch/PVA electrospun nanoscaffolds. Physicochemical characterizations confirmed the preservation of CuO's monoclinic crystalline structure and strong interactions between nanoparticles and polymer matrices, contributing to improved thermal stability and uniform fibrous morphology. The embedded CuO NPs exhibited well-dispersed nanoscale dimensions, facilitating enhanced bioavailability within the scaffold framework. Importantly, the developed nanocomposites exhibited superior anticancer activity against HT-29 and MCF-7 cell lines compared to individual components, indicating synergistic effects from nanoparticle-polymer integration. These findings highlight the potential of these biogenic CuO-loaded starch/PVA nanoscaffolds as promising candidates for anticancer therapeutics. Future research should focus on elucidating the molecular mechanisms underlying their cytotoxic effects and evaluating their performance in *in vivo* cancer models to advance clinical applicability. Overall, this study paves the way for eco-friendly, effective nanomaterial-based cancer treatments.

Ethics declaration: Not Applicable

Funding Declaration: Not Available

Conflicts of Interest: The authors declare no conflicts of interest.

Data Availability Statement: The full dataset of physiochemical characterization associated with this work is published in Mendeley Data (doi: 10.17632/mmyv8mmkbx.2). **Disclosure:** The material characterization data and figures (e.g., UV, SEM, FTIR, XRD, TGA, Zeta Potential and particle sizer) presented here were generated from a common dataset and are being reused across multiple related studies on nanomaterials. All biological and environmental analyses and conclusions are original to each manuscript.

REFERENCES

[1] Ganesan A, Kumar NG, Natarajan PM. Anticancer activity of silver nanoparticles synthesized from aqueous leaf extract of Solanum trilobatum (Purple fruit pea eggplant) on human oral cancer cells. Journal of Herbmed Pharmacololgy. 2024; 13(2): 260-268.

[2] Umapathy V, Dhanavel A, Kesavan R, Natarajan PM, Bhuminathan S, Vijayalakshmi P. Anticancer Potential of the Principal Constituent of Piper nigrum, Piperine: A Comprehensive Review. Cureus. 2024; 16(2): e54425.

[3] Umapathy VR, Swamikannu B, Natarajan PM, Devi R, Nandini MS, Vimalarani, Vijayalakshmi P. In Silico Molecular Docking of Ocimum sanctum Phytochemicals: Targeting Key Biomarkers in Oral Cancer. Journal of Pharmacy and Bioallied Sciences. 2024; 16(5): S4792-S4799.

[4] Swamikannu B, Umapathy VR, Natarajan PM, Nandini MS, Stylin AGSQ, Vimalarani V, Rajinikanth S. Unlocking the Therapeutic Benefits of Artemisia Annua: A Comprehensive Overview of its Medicinal Properties. Journal of Pharmacy and Bioallied Sciences. 2024; 16(5): S4248-S4253.

[5] Yadalam PK, Arumuganainar D, Natarajan PM, Ardila CM. Artificial intelligence-powered prediction of AIM-2 inflammasome sequences using transformers and graph attention networks in periodontal inflammation. Scientific Reports. 2025; 15: 8733.

[6] Yadalam PK, Chatterjee S, Natarajan PM, Ardila CM. Comparison of light gradient boosting and logistic r egression for interactomic hub genes in Porphyromonas gingivalis and Fusobacterium nucleatum-induced periodontitis with Alzheimer's disease. Frontiers in Oral Health. 2025; 6:1463458.

[7] Yadalam PK, Natarajan PM, Ardila CM. Variational graph autoencoder for reconstructed transcriptomic data associated with NLRP3 mediated pyroptosis in periodontitis. Scientific Reports. 2025; 15: 1962.

[8] Daniel Raja FS, Abraham L, Rangasamy K, Saikia K, Rathankumar AK, Mironescu M, Mironescu I, Palanisamy CP, Kanniappan GV. Next-Generation Microbiome Therapeutics: Psychobiotics and Fecal Microbiota Transplants (FMT) for Mental Health Treatment. Frontiers in Cellular and Infection Microbiology. 2026; 16: 1719357.

[9] Dharmaprakash S, Gunasekaran VP, Sivaramakrishnan R, Kanniappan GV, Jayaraman S, Mironescu M, Rajabathar JR, Mironescu ID, Palanisamy CP. Marine macroalgae-mediated ultrasonic-assisted green synthesis of CuO nanoparticles embedded in starch/PVA electrospun nanoscaffolds for in vitro α-amylase and α-glucosidase inhibitory activity. Scientific Reports. 2026.

[10] Surendran N, Chandrasekaran G, Raju MV, Chandrasekaran MK, Ahalliya RM, Palanisamy CP, Kanniappan GV, Arcot R, Alharbi NS, Thiruvengadam M. Anti-inflammatory potential of ethanolic extract of Maranta arundinacea L.: Insights from COX-2 modulation and oxidative stress analysis. South African Journal of Botany. 2026; 195: 142-151.

[11] Pei J, Senthilkumar MV, Hessini K, Subramaniyam S, Sivaramakrishnan R, Kanniappan GV, Jayaraman S, Palanisamy CP. Green fabrication of starch/PVA/CuO nanoscaffolds using marine macroalgae extract for enhanced anti-inflammatory activity. Sustainable Chemistry and Pharmacy. 2026; 51: 102397.

[12] Balasubramanian V, Loganathan L, Muthuswamy K, Viswanathan TM, Raju MV, Chandrasekaran MK, Ahalliya RM, Poorasamy J, Palanisamy CP, Dominic S, Kanniappan GV. Anticancer therapeutic efficacy of PEGylated β-galactosidase from Aspergillus terreus in DMBA-induced breast cancer: Toxicological, molecular and histopathological evaluation in Wistar rats. International Journal of Biological Macromolecules. 2026; 360: 151856.
[13] Jayaraman S, Eswaran A, Rajagopal P, Palanisamy CP, Veerakumar P, Veeraraghavan VP, Sirasanagandla SR. Neuroendocrine-associated epigenetic factors in cellular senescence: mechanisms and therapeutic implications. Biogerontology. 2026; 27(2): 64.
[14] Ponnusamy B, Rajagopal P, Palanisamy CP, Veeraraghavan VP, Jayaraman S. Mechanistic Exploration of the anticancer activity of Justicia adhatoda Plant Leaf Ethanolic Extract against Colon Cancer Cells: An in silico and in vitro Approach. Asian Pacific Journal of Cancer Prevention. 2026; 27(3): 1069-1080.
[15] Pei J, Saran VS, Sivaramakrishnan R, Kanniappan GV, Pandurangan V, Jayaraman S, Dhayalan VK, Mironescu M, Mironescu ID, Palanisamy CP. Ultrasonic-assisted, Sargassum ilicifolium (brown marine macroalgae)-mediated biogenic synthesis of CuO nanoparticles incorporated in starch/PVA electrospun nanoscaffolds: In vitro safety and antioxidant efficacy assessment. Bioorganic Chemistry. 2026; 173: 109679.
[16] Raj MAPA, Subramaniyam S, Kanniappan GV, Jayaraman S, Palanisamy CP. Sustainable fabrication of starch/PVA/CuO electrospun nanoscaffolds from Turbinaria ornata (marine macroalgae) extract: Physicochemical characterization and antidiabetic evaluation. Kuwait Journal of Science. 2026; 53(2): 100545.
[17] Pei J, Ganesh NS, Subramaniyam S, Sivaramakrishnan R, Kanniappan GV, Jayaraman S, Palanisamy CP. Sustainable fabrication of starch/PVA/CuO electrospun nanoscaffolds from Padina tetrastromatica (Brown macroalgae) extract: Physicochemical characterization and antidiabetic assessment. Sustainable Chemistry One World. 2026; 9: 100195.
[18] Sakthiraj A, Sivaramakrishnan R, Subramaniyam S, Kanniappan GV, Pandurangan V, Jayaraman S, Dhayalan VK, Mironescu M, Mironescu ID, Palanisamy CP. Starch/PVA electrospun nanoscaffolds loaded with ultrasonic-assisted green-synthesis of CuO nanoparticles from marine macroalgae (Gracilaria corticata) extract: Cytotoxicity and antioxidant analysis. Chemical Physics Impact. 2026; 12: 101018.
[19] Raju M, Chandrasekaran MK, Loganathan L, Ahalliya RM, Mironescu M, Mironescu ID, Palanisamy CP, Kanniappan GV. Lipid remodeling and ferroptosis in phosphatidylcholine-mediated tumor–stroma crosstalk. Frontiers in Molecular Biosciences. 2026; 13: 1742305.
[20] Kunamalla R, Panagal M, Palanisamy CP. Biogenic synthesis and fabrication of starch/PVA/CuO electrospun nanoscaffolds from Sargassum ilicifolium (brown marine macroalgae) extract for anticancer activity on HT-29 and MCF-7 cancer cells. Biocatalysis and Agricultural Biotechnology. 2026; 72: 103923.
[21] Pei J, Govindaraj H, Sivaramakrishnan R, Kanniappan GV, Pandurangan V, Dhayalan VK, Mironescu M, Mironescu ID, Jayaraman S, Palanisamy PC. Sustainable fabrication of biopolymer-based (starch/PVA) nanoscaffolds loaded with green-synthesized CuO nanoparticles from Sargassum wightii (marine macroalgae): Cytocompatibility and antioxidant activity. Biomaterials Advances. 2026; 182: 214660.
[22] Pei J, Perumal NC, Meng P, Long Q, Palanisamy CP. Extracellular vesicle-based biosensors for Alzheimer's disease: A new frontier in precision diagnostics. Ageing Research Reviews. 2026; 113: 102904.
[23] Shree P, Sivaramakrishnan R, Kanniappan GV, Pandurangan V, Jayaraman S, Dhayalan VK, Mironescu M, Mironescu ID, Palanisamy CP. Antioxidant and biocompatible CuO-starch/PVA nanoscaffolds via ultrasonic green synthesis using Turbinaria conoides (brown marine macroalgae). Medicine in Drug Discovery. 2025; 28: 100238.
[24] Gong J, Lin J, Guan T, Pei J, Palanisamy CP, El-AtyFrom AMA. selenium tolerance to nanoplastic antagonism: Comprehensive characterization of L. casei SNUT1 and its extracellular vesicle–nanoselenium complex. Food Bioscience. 2025; 74: 107749.
[25] Poochi SP, Sundarraj R, Raju MV, Chandrasekaran MK, Ahalliya RM, Palanisamy CP, Kanniappan GV, Kondapavuluri BK, Thiruvengadam M. Harnessing Nature: Computational and Experimental Insights Into *Ipomoea obscura* Metabolites for Bladder Cancer Therapy. Chemistry and Biodiversity. 2025; 0: e00909.
[26] Dugganaboyana GK, Kannankumar MKG, Shivaramakrishna S, Raju MV, Chandrasekaran MK, Ahalliya RM, Panneerselvam N, Palanisamy CP, Kanniappan GV. Phytochemical insights, antioxidant activity and therapeutic potential of Cassia senna against prostate cancer in Wistar albino rats. Discover Applied Sciences. 2025; 7:1206.
[27] Natarajan SR, Krishnamoorthy R, Alshuniaber MA, Gatasheh MK, Rajagopal P, Veeraraghavan VP, Palanisamy CP, Jayaraman S. KDM1A Facilitates Oncogenic Potential in Colorectal Cancer Progression Through the Activation of AXIN/GSK3β/β-Catenin Signaling Pathways: Evidence From Integrated Transcriptomics and In Vitro Studies. The Journal of Gene Medicine. 2025; 27(11): e70053.
[28] Guan T, Gong J, Lin J, Palanisamy CP, Jinjin Pei J, El-Aty AMA. Machine learning-driven multimodal optimization of selenium biotransformation and flavor profiling in fermented apple–Yacon functional beverages. Innovative Food Science & Emerging Technologies. 2025; 105: 104198.
[29] Natarajan SR, Krishnamoorthy R, Alshuniaber MA, Alsulami TS, Gatasheh MK, Rajagopal P, Palanisamy CP, Govindan R, Veeraraghavan VP, Jayaraman S. ABCE1 facilitates tumour progression via aerobic

glycolysis and inhibits cell death in human colorectal cancer cells through the p53 signalling pathway. Scientific Reports. 2025; 15: 24674.
[30] Huang Y, Guo H, Liu Y, Jin W, Palanisamy CP, Pei J, Oz F, El-Aty AMA. Effects of Natural Polysaccharides on the Gut Microbiota Related to Human Metabolic Health. Molecular Nutrition & Food Research. 2025; 69:e202400792.
[31] Poornima K, Meenakshi K.C, Manikandan V.R, Shankari G, Prabhu D, Rathi M.A, Palanisamy CP, Balaji R, Gopalakrishnan V.K. Exploring the anticancer potential of Jerantinine A from *Tabernaemontana coronaria* against prostate, breast, and ovarian cancers: A computational approach. *Journal of Complementary and Integrative Medicine*, 2025 22(2): 363–372.
[32] Palanisamy CP, Poompradub S, Sansanaphongpricha K, Jayaraman S, Subramani K. Faridah Sonsudin gGreen synthesis of Nigella sativa-mediated silver nanoparticles for enhanced antibacterial activity and wound healing: Mechanistic insights and biomedical applications. Environmental Nanotechnology, Monitoring & Management. 2025; 24: 101085.
[33] Surendran N, Raju MV, Chandrasekaran MK, Ahalliya RM, Palanisamy CP, Chandrasekaran G, Kanniappan GV. Physicochemical characterization of starch from Maranta arundinacea L.(arrowroot) rhizomes and its inhibition of COX-2: In vivo validation. Bioactive Carbohydrates and Dietary Fibre. 2025; 33: 100465.
[34] Kannappan P, Chandrasekaran MK, Raju MV, Gopalakrishnan S, Dhamodharan P, Ahalliya RM, Palanisamy CP, Raju B, Kanniappan GV. Exploring the anticancer potential of Jerantinine A from Tabernaemontana coronaria against prostate, breast, and ovarian cancers: a computational approach. Journal of Complementary and Integrative Medicine. 2025; 22(02): 363-372.
[35] Pei J, Kumarasamy RV, Jayaraman S, Kanniappan GV, Long Q, Palanisamy CP. Quercetin-functionalized nanomaterials: Innovative therapeutic avenues for Alzheimer's disease management. Ageing Research Reviews. 2025; 104: 102665.
[36] Jayaraman S, Prasad M, Natarajan SR, Krishnamoorthy R, Alshuniaber MA, Gatasheh MK, Veeraraghavan VP, Rajagopal P, Palanisamy CP. Molecular mechanisms underlying the effects of beta-sitosterol on TGF-β1/Nrf2/SIRT1/p53-mediated signaling in the kidney of a high-fat diet and sucrose-induced type-2 diabetic rat. Chemico-Biological Interactions. 2025; 411: 111443.
[37] Huang Y, Guo H, Liu Y, Jin W, Palanisamy CP, Pei J, Oz F, El-Aty AMA. Effects of Natural Polysaccharides on the Gut Microbiota Related to Human Metabolic Health. Molecular Nutrition & Food Research. 2025; e202400792.
[38] Natarajan PM. Dental Bioinformnatics-Current Scope and Future perspectives. Research Journal of Pharmacy and Technology. 2022;15(5):2351-6.
[39] Natarajan PM, Umapathy VR, Murali A, Swamikannu B. (2022). Computational Simulations of Identified marine-derived Natural Bioactive Compounds As Potential Inhibitors of Oral Cancer. Future Science OA. 2022; 8(3).
[40] Natarajan PM, Umapathy VR. Role of transcriptomics in the study of oral cancer. Frontiers in Oral Health. 2025; 6:1524364.
[41] Natarajan PM, Swamikannu B, Sivaraman NM, Stylin AGSQ. Prevention of Oral Cancer: A Comprehensive Guide. Journal of Pharmacy and Bioallied Sciences. 2024; 16(5): S4239-S4241.
[42] Natarajan PM. Computational Studies on Recent Congeners of Fluoroquinolones and Nitroimidazoles for Their Use in Periodontal Therapy. Journal of Pharmacy and Bioallied Sciences. 2024; 16(5): S4731-S4740.
[43] Natarajan PM, Bhuminathan S, Rajan R, Bindu K, Loganathan K, Veerakumar R. The Crucial Role of Smoking Cessation in Preventing Oral Cancer. Journal of Pharmacy and Bioallied Sciences. 2024; 16(5): S4245-S4247.
[44] Natarajan PM, Bhuminathan S, Leela B, Bindu K, Loganathan K, Ramachandran V. Smoking and its Role in Oral Cancer. Journal of Pharmacy and Bioallied Sciences 16(5): S4242-S4244.
[45] Vidhyarekha U, Natarajan PM, Bhuminathan S, Sabarinathan J, Suba R, Vijayalakshmi P. Role of artificial intelligence in Oral Cancer. Advances in Public Health. 2024. 2024: 3664408.
[46] Ganesan A, Kumar NG, Natarajan PM, Gauthaman J. Automated classification of elongated styloid processes using deep learning models-an artificial intelligence diagnostics. Frontiers in Oral Health. 2025; 5: 1424840.
[47] Umapathy VR, Natarajan PM, Swamikannu B. Regenerative Strategies in Dentistry: Harnessing Stem Cells, Biomaterials and Bioactive Materials for Tissue Repair. Biomolecules. 2025; 15: 546.
[48] Ganesan A, Kumar NG, Natarajan PM. Solanum trilobatum leaf extract-derived silver nanoparticles downregulate the PI3K/AKT/mTOR signaling pathway and attenuate oral squamous cell carcinoma cell proliferation. Journal of Herbmed Pharmacology. 2024; 13(2): 300-307.
[49] Perumal MKK, Renuka RR, Subbiah SK, Natarajan PM. Artificial intelligence-driven clinical decision support systems for early detection and precision therapy in oral cancer: a mini review. Frontiers in Oral Health. 2025; 6: 1592428.
[50] Ramesh E, Ganesan A, Lakshmi KC, Natarajan PM. Artificial intelligence-based diagnosis of oral leukoplakia using deep convolutional neural networks Xception and MobileNet-v2. Frontiers in Oral Health. 2025; 6: 1414524.

[51] Prabhakaran P, Palanisamy CP, Shanmugam A, Damodharan P, Swaminathan H, Devaraj D, Ahalliya RM, Kanniappan GV. Isolation, structural characterization, and molecular docking studies on the bioactive compound from n-Hexane extract of Emilia sonchifolia (L.) DC against the pancreatic cancer target Aurora 2 Kinase. Journal of Complementary and Integrative Medicine. 2024; 22(1): 0290.
[52] Jiang H, Kumarasamy RV, Pei J, Raju K, Kanniappan GV, Palanisamy CP. Integrating engineered nanomaterials with extracellular vesicles: Advancing targeted drug delivery and biomedical applications. Frontiers in Nanotechnology. 2024; 6: 1513683.
[53] Guo H, Liu Y, Wan T, Song D, Palanisamy CP, Geng J, Pei J, Özmen S, El-Aty AMA. Toward personalized cancer management: Role of precision nutrition–diet interventions. Journal of Functional Foods. 2024; 123: 106584.
[54] Natarajan SR, Krishnamoorthy R, Alshuniaber MA, Al-Anazi KM, Farah MA, Rajagopal P, Palanisamy CP, Veeraraghavan VP, Jayaraman S. Identification of FOXM1 as a novel protein biomarker and therapeutic target for colorectal cancer progression: Evidence from immune infiltration and bioinformatic analyses. International Journal of Biological Macromolecules. 282 (Part 4): 137201.
[55] Rajendran MS, Jayaraman S, Khan JM, Jasmine S, Prabhakaran RK, Raju MV, Chandrasekaran MK, Ahalliya RM, Kannappan P, Palanisamy CP, Kanniappan GV. Investigating the colon toxicity and carcinogenic role of monosodium glutamate compared with Dimethylhydrazine in male Wistar rats: Exploring the link to childhood colon cancer risk. Journal of King Saud University - Science. 2024; 36(11): 103507.
[56] Kumarasamy RV, Natarajan P, Umapathy VR, Roy JR, Rab SO, Saeed M, Panagal M, Mironescu M, Srinivasan GP, Palanisamy CP. Clinical Applications and Therapeutic Potentials of Advanced Nanoparticles: A Comprehensive Review on Completed Human Clinical Trials. Frontiers in Nanotechnology. 2024; 6:1479993.
[57] Jin W, Pei JJ, Roy JR, Jayaraman S, Ahalliya RM, Kanniappan GV, Mironescu M, Palanisamy CP. Comprehensive review on single-cell RNA sequencing: A new frontier in Alzheimer's disease research. Ageing Research Reviews. 2024; 274: 102454.
[58] Pei J, Palanisamy CP, Jayaraman S, Natarajan PM, Umapathy VR, Roy JR, Panagal M, Jayaraman S. Curcumin-loaded polymeric nanomaterials as a novel therapeutic strategy for Alzheimer's disease: A comprehensive review. Ageing Research Reviews. 2024; 99: 102393.
[59] Pei J, Palanisamy CP, Jayaraman S, Natarajan PM, Umapathy VR, Roy JR, Thalamati D, Ahalliya RM, Kanniappan GV, Mironescu M. A comprehensive review on starch-based Sustainable Edible Films Loaded with Bioactive Components for Food Packaging. International Journal of Biological macromolecules. 2024; 274 (Part-1): 133332.
[60] Palanisamy CP, poompradub S, Sansanaphongpricha K, Subramani K, Sonsudin F. Increased expression levels of PDGF and VEGF magnify the wound healing potential facilitated by biogenic synthesis of silver nanoparticles. Nano-Structures & Nano-Objects. 2024; 39: 101236.
[61] Pei J, Palanisamy CP, Jayaraman S, Natarajan PM, Umapathy VR, Roy JR, Thalamati D, Ahalliya RM, Kanniappan GV, Mironescu M. Proteomics Profiling of Extracellular Vesicle for Identification of Potential Biomarkers in Alzheimer's Disease: A Comprehensive Review. Ageing Research Reviews. 2024; 99: 102359.
[62] Xi J, Wang T, Xian P, Liu X, Du M, Yang H, Palanisamy CP, Lin W, Long Q. Proteomic insights uncover enhanced neurotherapeutic potential in conditioned mesenchymal stem cell-derived extracellular vesicles. Extracellular Vesicle. 2024; 3: 100037.
[63] Pei J, Natarajan PM, Umapathy VR, Swamikannu B, Sivaraman NM, Krishnasamy L, Palanisamy CP. Advancements in the synthesis and functionalization of zinc oxide-based nanomaterials for enhanced oral cancer therapy. Molecules. 2024; 29(11): 2706.
[64] Gatasheh MK, Natarajan SR, Krishnamoorthy R, Alsulami TS, Rajagopal P, Palanisamy CP, Veeraraghavan VP, Jayaraman S. Molecular analysis to identify novel potential biomarkers as drug targets in colorectal cancer therapy: an integrated bioinformatics analysis. Molecular and Cellular Oncology. 2024; 11(1): 2326699.
[65] Pei J, Yan Y, Jayaraman S, Rajagopal P, Natarajan PM, Umapathy VR, Gopathy S, Roy JR, Sadagopan CS, Thalamati D, Palanisamy CP, Mironescu M. A review on advancements in the application of starch-based nanomaterials in biomedicine: Precision drug delivery and cancer therapy. International Journal of Biological Macromolecules. 2024; 130746.
[66] Pei JJ, Yan Y, Palanisamy CP, Jayaraman S, Natarajan PM, Umapathy VR, Gopathy S, Roy JR, Sadagopan JC, Thalamati D, Mironescu M. Materials-based drug delivery approaches: Recent advances and future perspectives. Green Processing and Synthesis. 2024; 13: 20230094.
[67] Pei JJ, Deng W, Liu Y, Guo Y, Chen J, Abdu H, Khan MR, Palanisamy CP, El-Aty AM. A Comprehensive Review of Cornus officinalis: Health Benefits, Phytochemistry, and Pharmacological Effects for Functional Drug and Food Development. Frontiers in Nutrition. 2023; 10: 1309963.
[68] Alugoju P, Palanisamy CP, Anthikapalli NVA, Jayaraman S, Prasanskulab A, Chuchawankul S, Dyavaiah M, Tencomnao T. Exploring the anti-aging potential of natural products and plant extracts in budding yeast Saccharomyces cerevisiae: A review. F1000Research. 2023; 12: 1265.

[69] Lavanya M, Krishnamoorthy R, Alshuniaber MA, Manoharadas S, Palanisamy CP, Veeraraghavan VP, Jayaraman S, Rajagopal P, Padmini R. Formulation, characterization and evaluation of gelatin-syringic acid/zinc oxide nanocomposite for its effective anticancer, antioxidant and anti-inflammatory activities. Journal of King Saud University-Science. 2023; 35: 102909.
[70] Palanisamy CP, Poompradub S, Sansanaphongpricha K, Jayaraman S, Subramani K, Sonsudin F. Biosynthesis of silver nanoparticles (AgNPs) using ethanolic extract of Nigella sativa (L.) seeds promotes wound healing via PDGF and VEGF signalling pathways activation. Biocatalysis and Agricultural Biotechnology. 2023; 54: 102970.
[71] Prasad M, Jayaraman S, Natarajan SR, Veeraraghavan VP, Krishnamoorthy R, Gatasheh MK, Palanisamy CP, Elrobh M. Piperine modulates IR/Akt/GLUT4 pathways to mitigate insulin resistance: Evidence from animal and computational studies. International Journal of Biological Macromolecules. 2023; 253: 127242.
[72] Palanisamy CP, Pei JJ, Phaniendra A, Venkata AAN, Jayaraman S, Veeraragahavan VP, Sridevi G, Roy JR, Janaki CS, Thalamati D, Mironescu M, Luo Q, Chai Y, Long Q. New Strategy of Neurodegenerative Disease Treatment with Extracellular Vesicles (EVs) Derived from Mesenchymal Stem Cells (MSCs). *Theranostics*. 2023; 13(12):4138-4165. doi:10.7150/thno.83066.